HiSST: 3rd International Conference on
High-Speed Vehicle Science & Technology
14 -19 April 2024, Busan, Korea

Numerical analysis of non-equilibrium effects using a Unified Solver

Seungyong Baeg[*], *Raghava S.C. Davuluri*[*], *and Alexandre Martin*[*†]

Abstract

Historically, efforts have been made to model the interaction between porous ablative material and hypersonic flow by coupling a computational fluid dynamics (CFD) solver to a material response solver. Here, a new unified approach is used where the Volume Averaged Navier-Stokes (VANS) equations are solved over both domains. Recent advances have demonstrated the ability of this approach to model simplified hypersonic flow. In this paper, the solver is updated to account for non-equilibrium thermochemistry. More specifically, the two-temperature model and the chemistry model are implmented, where nonequilibrium thermochemical effects on gas flow are studied. Thermochemistry heat bath simulations are used to validate the VANS approach on chemical and thermal relaxation. A new phenomenological relaxation time is proposed so that thermal equilibrium is achieved at the surface of the solid, as would be the case with pure CFD simulations. With this new model, the final equilibrium temperature, mass fraction, and mole fraction show good agreement with the reference data.

Keywords: *non-equilibrium, ablation, thermal protection system, thermo-chemistry*

Nomenclature

S	source term	ϕ	porosity
t	time, s	M	molar weight, g/mol
i	index of gas species	R_u	universal gas constant, J/mol·K
s_i	index of solid species	n	number density, $1/m^3$
T_{tr}	translational-rotational temperature, K	X	mass fraction
T_{ve}	vibrational-electronic temperature, K	Y	mole fraction
τ	relaxation time, s		

1. Introduction

During the planetary mission, space vehicle encounters high heat fluxes during atmospheric entry situation. The high enthalpy flow over the vehicle can damage the structure and is equipped with a Thermal Protection System (TPS) to protect its integrity. Ablative materials are most commonly used TPS materials for planetary mission which undergo mass removal mechanisms to counter the heat fluxes. It is necessary to accurately predict the response of the material to high heat for designing a cost efficient TPS that provides safety to the crew by successfully entering the planetary atmosphere. On the computational front, some studies were conducted that focused on the interaction between ablative material and hypersonic flow. These simuations can be categorized into four methods [1]: uncoupled approach, weekly coupled approach, strongly soupled approach, and unified approach. At first, the uncoupled approach considers gas- and solid-region separated ones by using a dedicated boundary condition for computing the surface ablation. Heat exchange and blowing at each surface are calculated using surface balance equations. As the dynamic interaction between both domains is not considered, the shape change is not considered. Second, the weakly coupled approach exchanges the information at intersection using mass and energy balance. The flow solver and material response solvers march in time differently, and each solver has different time scales, and the information exchange is performed only at the dedicated time steps. Third, the strongly coupled approach solves both domains at the same time

[*] *Mechanical and Aerospace Engineering, University of Kentucky, Lexington, KY, USA*
[†] *Correspondance: alexandre.martin@uky.edu*

steps, and additional surface balance treatments are needed to exchange mass and energy between two regions. Lastly, the unified approach solves both the gas region and the solid region at the same time as both regions are in the single domain. This method does not require implementation of surface balance equations and additional boundary conditions at the intersection, as it solves two regions seamlessly, and interface exchange is resolved with a global set of equations which is applicable for both regions. The researches for this method have performed recently. Schrooyen et al. [2, 3] developed the solver, which uses a unified domain, and validated it by comparing it with the flow tube oxidation experiment. Duzel et al. [1, 4] developed a Universal Solver (US) module for Kentucky Aerothermodynamics and Thermal-response System (KATS) [5, 6, 7] which solves the fluid domain and solid domain with a set of equations. The model does not require any moving mesh algorithm to track and exchange the variables at the interface. Baeg et al. [8] implemented a thermal non-equilibrium model on KATS-US and the non-equilibrium effects at the gas-surface interface are numerically studied. However, previous research does not account for the thermochemistry effect, which is one of the key points of hypersonic phenomena. For this reason, the present work aims to construct a non-equilibrium thermochemistry effect for KATS-US, and the recent functionalities and its results are discussed in this paper.

2. Numerical approach

2.1. Two-temperature model

The energy of gas species is summation of four energy modes [9]:

$$e_i = e_{tran,i} + e_{rot,i} + e_{vib,i} + e_{elec,i} + h_s^0, \tag{1}$$

where $e_{tran,i}$ is the translational energy, $e_{rot,i}$ is the rotational energy, $e_{vib,i}$ is the vibrational energy, $e_{elec,i}$ is the electronic energy, and h_s^0 is the enthalpy of formation. This can be divided into two part, $e_{tr,i}$ and $e_{ve,i}$ given as:

$$e_{tr,i} = e_{tran,i} + e_{rot,i} + h_s^0, \tag{2}$$

$$e_{ve,i} = e_{vib,i} + e_{elec,i}. \tag{3}$$

e_{tr} is function of T_{tr}, and e_{ve} is function of T_{ve}. The detail information regarding the energy equation for each energy mode is detailed in Refs. [9, 10, 8].

2.2. Chemistry model

The general chemical reaction can be described by:

$$\sum_{i=1}^{ns} \alpha_{i,r} A_i = \sum_{i=1}^{ns} \beta_{i,r} B_i, \tag{4}$$

where α, and β denote the stoichiometric coefficient of reactants and products respectively. A, and B represent the gas species of reactants and products respectively. i is the index of gas species, and r is the index of each reactions. In this research, Park's two-temperature model is implemented[11]. Translational-rotational temperature, T_{tr}, and vibrational-electronic temperature, T_{ve} control the dissociation in this model. The forward temperature of this model can be formulated as:

$$T_f = T_{tr}^{a_f} T_{ve}^{b_f}. \tag{5}$$

For a_f, and b_f are usually given as $a_f = 0.5$ and $b_f = 0.5$, or $a_f = 0.7$ and $b_f = 0.3$[10]. The forward reaction rate can be calculated using:

$$k_{fr} = A_f T_f^{\eta_r} \exp(-T_{ar}/T_f), \tag{6}$$

where A_f, η, and activation temperature, T_{ar}, are empirical coefficients for Arrhenius curve fit. The backward temperature is defined as:

$$T_b = T_{tr}^{a_b} T_{ve}^{b_b}. \tag{7}$$

For dissociation reaction, $a_b = 1$, and $b_b = 0$ in this model. The backward reaction rate can be calculated using:

$$k_{br}(T_b) = \frac{k_{fbr}(T_b)}{K_{cr}(T_b)}. \tag{8}$$

where k_{fbr} is given by:

$$k_{fbr} = A_f T_b^{\eta_r} \exp(-T_{ar}/T_b). \tag{9}$$

The equilibrium constant K_{cr} can be calculated by using Gibb's free energy[12].

$$\log K_{cr} = -\sum_{i=1}^{ns} \frac{(\beta_{i,r} - \alpha_{i,r})\hat{g}_i(T_b)}{R_u T_b} - \log(R_u T_b) \sum_{i=1}^{ns} (\beta_{i,r} - \alpha_{i,r}), \tag{10}$$

where $\hat{g_i}$ is the Gibbs energy per unit mole of the species and it can be described as Eq. 11.

$$\hat{g_i} = \hat{h_i} - T_b \hat{s_i}, \tag{11}$$

where $\hat{h_i}$ is the enthalpy of the species per unit mole, and $\hat{s_i}$ is the entropy of the species per unit mole. The chemical production rate of the gas species of each reaction can be described as Eq. 12.

$$\dot{\omega}_{i,r} = (\beta_{i,r} - \alpha_{i,r}) \left[k_{fr} \times 10^3 \prod_{j=1}^{ns} (\frac{\rho_j}{M_j} \times 10^{-3})^{\alpha_{j,r}} - k_{br} \times 10^3 \prod_{j=1}^{ns} (\frac{\rho_j}{M_j} \times 10^{-3})^{\beta_{j,r}} \right], \tag{12}$$

where j is the jth species in the reaction. It should be noted that centimeter-gram unit system which is generally used in the calculation of chemical reactions [10]. The factor 10^{-3} converts meter-kilogram unit to centimeter-gram unit system. And the factor 10^3 converts it to meter-kilogram unit system again. The net mass rate of production of the each species is given by

$$\dot{\omega}_i = M_i \sum_r \dot{\omega}_{i,r}, \tag{13}$$

where M_i denotes the molar mass of the species.

2.3. Source term

The vibrational-electronic energy source term, S_{ve}, should account multiple energy exchange mechanisms. All of these energy exchange mechanisms occur in a molecular level. The total vibrational-electronic energy source term is described as

$$S_{ve} = S_{cv} + S_{tv}, \tag{14}$$

where S_{cv} represents the vibrational-electronic energy created or removed by chemical reaction rates, there are two types of models for S_{cv}, preferential model and non-preferential model. The preferential model is given as Eq. 15 which assumes that dissociation and recombination of molecules occur in higher vibrational states.

$$S_{cv} = \sum_{i=1}^{ngs} \alpha D_i(e_{ve,i}), \tag{15}$$

where $\alpha = 0.3$, and D_i is the dissociation potential of the molecule. Non-preferential model is employed for chemistry model assuming that molecules are created and consumed at the average vibrational energy [10], and S_{cv} is given as

$$S_{cv} = \sum_{i=1}^{ngs} \dot{\omega}_i(e_{ve,i}). \tag{16}$$

S_{tv} represents energy exchange between translational-rotational energy, E_{tr}, and vibrational-electronic energy, E_{ve}. It is constructed in KATS-US for previous research to account for the non-equilibrium effect of hypersonic flow [8]. The energy exchange between translational-rotational and vibrational-electronic energy modes, S_{tv}, is modeled based on the relations proposed by Landau-Teller[13]. The energy exchange rate is

$$S_{tv} = \sum_{i=1}^{ngs} \rho_i \frac{e^*_{ve,i} - e_{ve,i}}{\tau_{gas+solid}}, \tag{17}$$

where $e^*_{ve,i}$ and $e_{ve,i}$ are defined as the vibrational-electronic energy of the species as a function of T_{tr} and T_{ve}, respectively, and τ_{i+s} is defined as the relaxation time of the control volume. In the present work, the relaxation time of the control volume is defined in Eq. 18 as:

$$\tau_{gas+solid} = \exp\left[\ln(\tau_{gas}) + \frac{1-\phi}{1-\phi_{solid}}(\ln(\tau_{solid}) - \ln(\tau_{gas}))\right] \tag{18}$$

where τ_{gas} and τ_{solid} are the relaxation times for gas species and solid in the control volume, ϕ and ϕ_{solid} are the porosities of the control volume and solid material, respectively. Detail information regarding the relaxation time is explained in the previous research [8].

3. Verification

The verification of two-temperature model in heat bath test cases is conducted. The computational domain is set as 1 mm^3 cube for every test cases in this research as shown in Fig. 1, and symmetry condition is applied to every boundary to make it adiabatic condition.

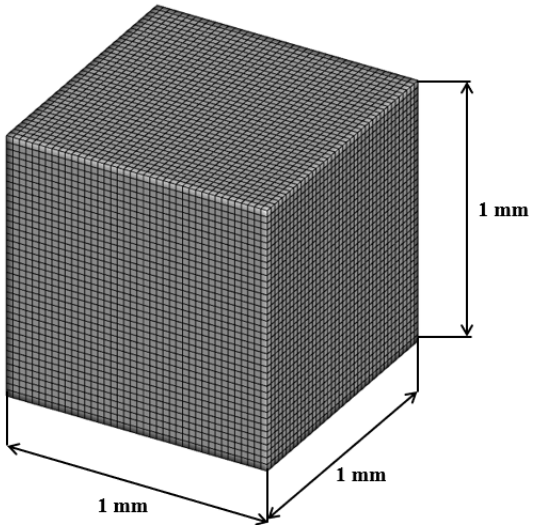

Fig 1. Computational domain of heat bath.

3.1. Gas heat bath

The results of KATS-US are compared with Boyd's results [14] and the results of Kentucky Aero-thermodynamics and Thermal-response System-CFD (KATS-FD). The validity of non-equilibrium effect in KATS-FD is verified by several references [6, 15, 10, 5, 7].The initial conditions are taken from Boyd et al. [14], and the single gas species N_2 is used for test cases. As the reference [14] does not consider electronic energy, both KATS-US and KATS-FD are run without considering electronic energy for the verification of heat bath test cases.

The vibrational heating ($T_{tr} > T_{ve}$) and the cooling ($T_{tr} < T_{ve}$) [14] test cases are conducted, and initial conditions are presented in Table 1. As shown in Fig. 2, KATS-US shows good agreement with the reference data [14],and the result of KATS-FD for both test cases. In case of the vibrational heating, it

reaches equilibrium state before 10^{-5} seconds while the the vibrational cooling reaches the equilibrium state after 10^{-5} seconds. KATS-US shows about 0.21% of relative error for vibrational heating and about 0.08% of relative error for vibrational cooling compared to the results of the reference [14].

Table 1. The initial conditions of gas heat bath test cases

Mode	T_{tr} [K]	T_{ve} [K]	P [Pa]
Heating	10,000	1,000	101,325
Cooling	3,000	10,000	101,325

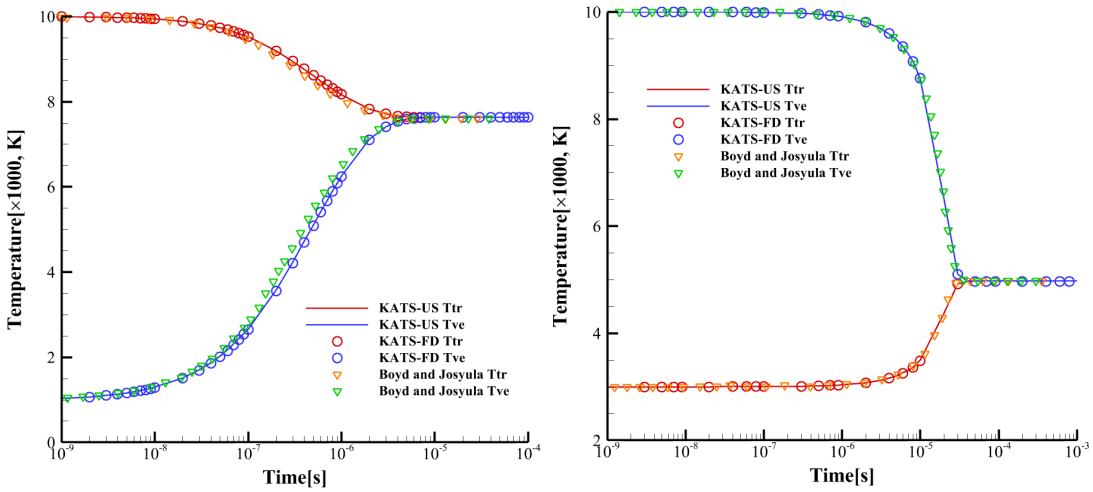

(a) The vibrational heating (b) The vibrational cooling

Fig 2. Temperature profile of gas heat bath.

3.2. Chemistry heat bath

Chemistry model in KATS-US is compared with the results of Casseau et al. [16]. According to the Refs. [16], the electronic energy is not considered, only irreversible molecule-molecule is considered as described in Eq. 19, and preferential model is adopted. Two verification test cases are conducted, the first test case is set as equilibrium state at the initial state, and the second test case is set as non-equilibrium state at the initial state, the initial conditions for these test cases are given as Table 2. For both test cases, $a_f = 0.7$, $b_f = 0.3$.

$$N_2 + N_2 \rightharpoonup 2N + N_2, \tag{19}$$

Table 2. The initial conditions of chemistry heat bath verification

Initial state	T_{tr} [K]	T_{ve} [K]	n_{0,N_2} [m^{-3}]	$n_{0,N}$ [m^{-3}]
Equilibrium	30,000	30,000	5×10^{22}	5×10^{22}
Non-equilibrium	30,000	1,000	5×10^{22}	5×10^{22}

As shown in Fig. 3, temperature and number density profiles agree well with the Ref. [16].

For the case of the non-equilibrium chemistry heat bath, T_{tr} shows good agreement. T_{ve} shows the biggest error around 10^{-6} seconds, and the maximum error is around 5.78%.

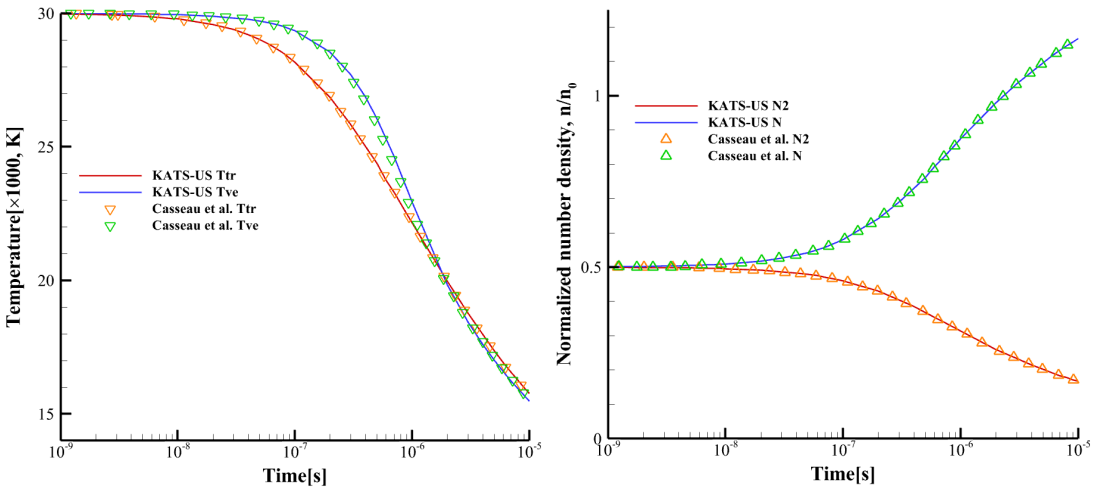

(a) Temperature profile (b) Number density profile

Fig 3. Equilibrium chemistry heat bath.

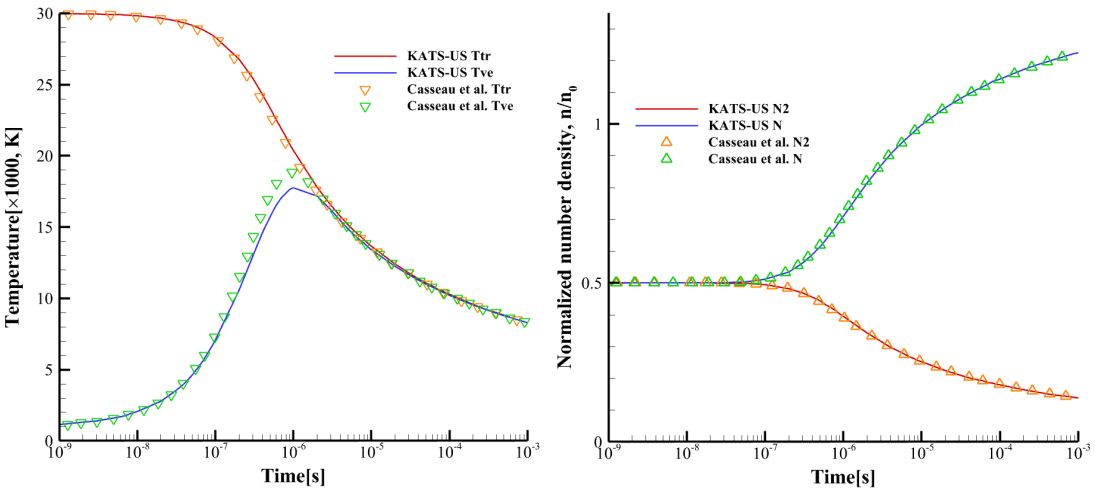

(a) Temperature profile (b) Number density profile

Fig 4. Non-Equilibrium chemistry heat bath.

4. Results and Discussion

4.1. Chemistry heat bath

The chemistry model in KATS-US is compared with the results of KATS-FD. The chemistry model in KATS-FD was previously verified, as can be seen in Refs [15, 10]. For this case – and the following ones as well – the two-species (N_2, N) chemical reaction model presented in Eq. 20 is used, and only gas chemistry heat bath is considered in this research. The a_f and b_f are all given 0.5, and a_b and b_b are given as 1 and 0 respectively, which means only T_{tr} is considered for the backward temperature while T_{tr} and T_{ve} are both considered for forward temperature. For the chemistry heat bath test cases, heat bath with equilibrium state at initial condition, and non-equilibrium state at the initial condition are conducted. However, the ionized flow is not considered, and only gas-chemistry heat bath simulation is considered in this research. The non-preferential model is adopted for these test cases.

$$\begin{aligned} N_2 + N_2 &\rightleftharpoons 2N + N_2, \\ N_2 + N &\rightleftharpoons 2N + N. \end{aligned} \tag{20}$$

The initial conditions for the first test case are described at Table 3.

Table 3. Chemistry heat bath with equilibrium state at initial state

T_{tr} [K]	T_{ve} [K]	P [Pa]	Y_{N_2}	Y_N
20,000	20,000	101,325	0.5	0.5

It starts with equilibrium temperature, which means that T_{tr} and T_{ve} are given the same value at the initial condition. As shown in Fig. 5, KATS-US shows good agreement with KATS-FD. The T_{tr} decreases till 10^{-5} seconds, and then starts to increase to reach the equilibrium state. As dissociation is an endothermic reaction, T_{tr} decreases more rapidly than T_{ve}. As shown in Fig. 6, both mass fraction and mole fraction show good agreement with the results of KATS-FD. These indicate that the N_2 molecules are broken down to N atoms as dissociation proceeds. This case reaches equilibrium state at around 10^{-4} seconds in terms of temperature, mass fraction, and mole fraction.

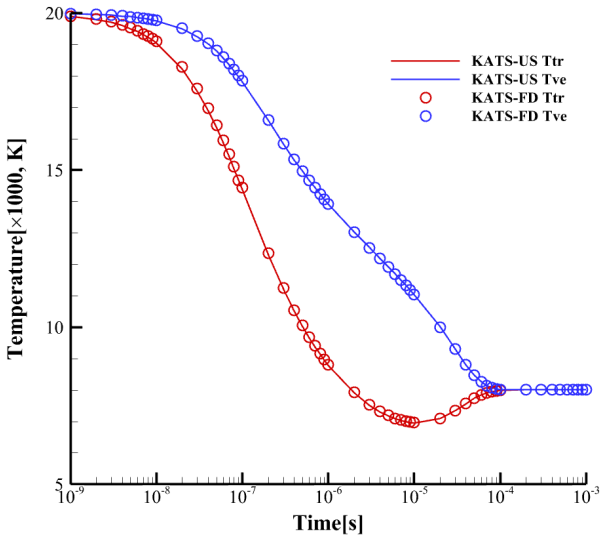

Fig 5. Temperature profile of the equilibrium chemistry heat bath

The initial conditions for the second test case are described in Table 4. It starts with non-equilibrium state which means T_{tr} and T_{ve} are not same at initial condition. As shown in Fig. 7, KATS-US shows good

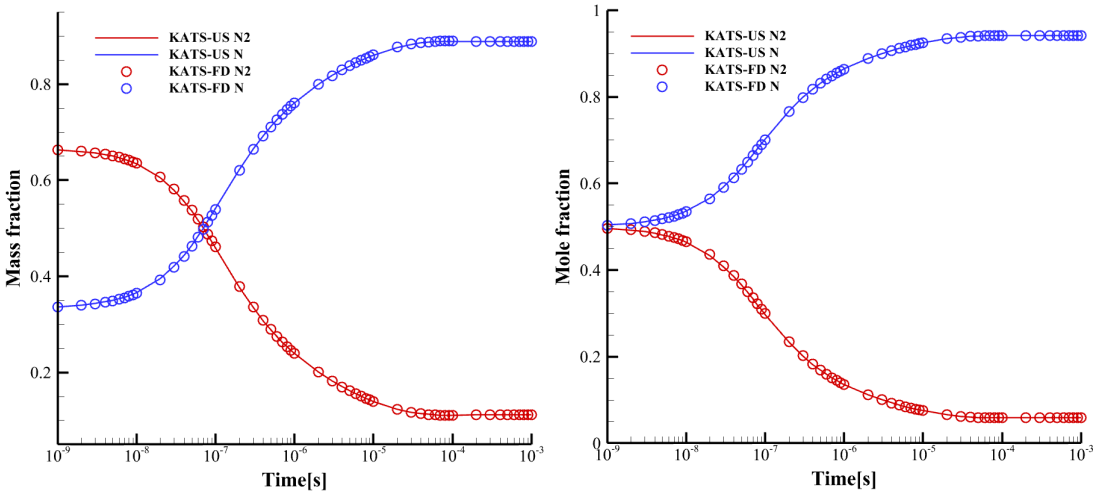

(a) Mass fraction profile (b) Mole fraction profile

Fig 6. Mass and mole fraction of the equilibrium chemistry heat bath.

agreement with the result of KATS-FD. The non-equilibrium chemistry heat bath test case shows both vibrational heating and vibrational cooling, while the equilibrium chemistry heat bath test case show only vibrational cooling. For the non-equilibrium chemistry heat bath test case, two-temperature heat bath (nonreacting) and chemistry heat bath (reacting) are compared to demonstrate the effect of chemical reaction. The non-reacting case takes less time to reach equilibrium state compared to reacting case. The final equilibrium temperature of the reacting case is lower than that of the non-reacting case due to dissociation. As shown in Fig. 8, KATS-US' results agree well with KATS-FD's results. This test case also shows the variation of mass and mole fraction as a result of dissociation reaction. This case reaches equilibrium state at around 10^{-4} seconds in terms of temperature, mass fraction, and mole fraction.

Table 4. Chemistry heat bath with non-equilibrium state at initial state

T_{tr} [K]	T_{ve} [K]	P [Pa]	Y_{N_2}	Y_N
30,000	1,000	101,325	0.5	0.5

4.2. Solid heat bath

Solid heat bath test case is conducted to investigate the non-equilibrium effect inside porous material. For the solid heat bath test case, vibrational heating and cooling are both considered, and the initial conditions are given as Table 5, and single species N_2 is used for working fluid.

Table 5. The initial conditions of solid heat bath test cases

Mode	T_{tr} [K]	T_{ve} [K]	P [Pa]	ρ_s [kg/m^3]	ϕ_s
Heating	5,000	1,000	101,325	179	0.87
Cooling	1,000	5,000	101,325	179	0.87

The τ_{solid} described in Eq. 18 is given as 10^{-13} when assumed as equilibrium state inside the porous material, and τ_{gas} which employs Landau-Teller equation [13] is used when it is assumed as non-equilibrium state inside the porous material. As shown in Fig. 9(a), vibrational heating and vibrational cooling reach equilibrium state almost at the same time as the relaxation time is given as constant. In case of the

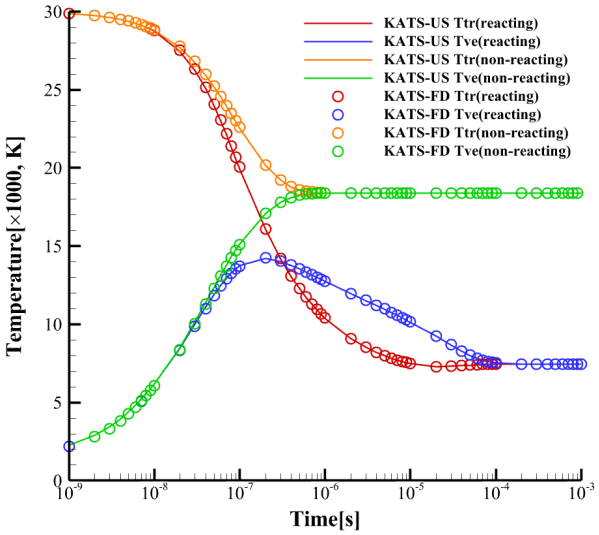

Fig 7. Temperature profile of the non-equilibrium chemistry heat bath

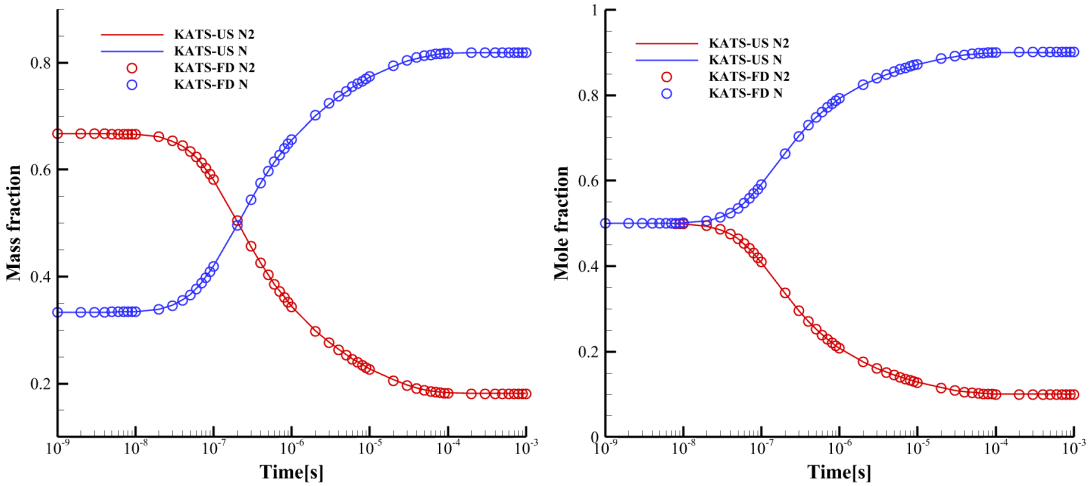

(a) Mass fraction profile (b) Mole fraction profile

Fig 8. Mass and mole fraction of the non-equilibrium chemistry heat bath.

non-equilibrium solid heat bath (Landau-Teller equation), vibrational heating and cooling show significant difference in relaxation time as shown in Fig. 9(b). Vibrational cooling takes much longer time for relaxation compared to vibrational heating when Landau-Teller equation [13] is employed.

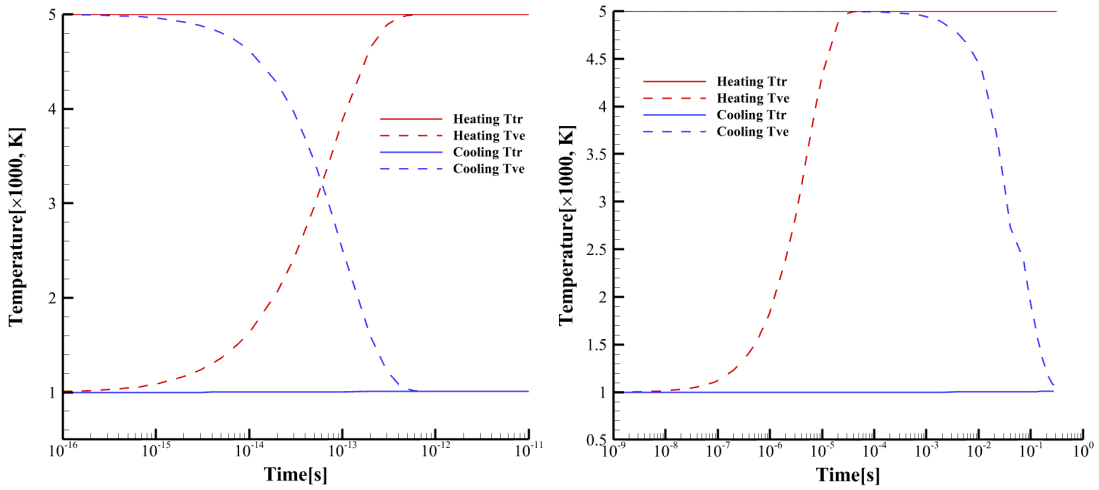

(a) Equilibrium solid heat bath (b) Non-equilibrium solid heat bath

Fig 9. Temperature profile of solid heat bath.

5. Conclusion

The KATS-US uses a single set of equations which are applicable for both the gas and the solid region of the problem. As both regions are modeled as a single domain, it does not require surface balance equations and boundary conditions at the interfaces between solid and gas. For the two-temperature heat bath cases with gas phase and porous media domain were carried out, respectively, and the gas heat bath showed good agreement with the reference data [14] for both vibrational heating and cooling. Vibrational heating took less time to reach equilibrium state than vibrational cooling. It is considered that this is because the effect of E_{ve} is very weak in the vibrational heating case while the effect of it is strong in the vibrational cooling case as T_{ve} of the vibration heating was relatively lower than the one of the cooling case at initial condition. The heat bath with porous media domain was conducted. By assuming the equilibrium state or the non-equilibrium state, each relaxation equation was employed, and the results were compared. When it was assumed as equilibrium state, the extremely low value of constant was used for relaxation time. The Landau-Teller equation was used when it was assumed to be a non-equilibrium state inside the porous material. For a non-equilibrium solid heat bath, vibrational cooling took much longer time to reach equilibrium state, which is unphysical. For this reason, a new equation is needed to account for the non-equilibrium effect inside the porous material. In the present work, heat bath chemistry test cases were conducted, and the results were compared with the KATS-FD results, which is an already verified code. For the first test case (equilibrium state at initial condition), a temperature drop was observed, since the dissociation is an endothermic reaction. The results showed good agreement with the KATS-FD's results. For the second test case (non-equilibrium state at the initial condition), it showed a lower equilibrium temperature when a chemistry model was implemented compared to the non-reacting case. For both equilibrium and non-equilibrium chemistry heat bath test cases, mass and mole fraction variation were observed and showed good agreement with the KATS-FD. As a future work, non-equilibrium effect inside the porous media will be accounted, and gas-surface chemistry will be investigated.

6. Acknowledgements

Financial support for this work was provided by NASA STRI Award 80NSSC21K1117.

References

[1] Duzel, U., *Development of universal solver for high enthalpy flows through ablative materials*, Ph.d. dissertation, University of Kentucky, Lexington, Kentucky, October 2020.

[2] Schrooyen, P., Hillewaert, K., Magin, T., and Chatelain, P., "Fully implicit integrated approach for the numerical simulation of aerothermal flows through and around ablative thermal protection systems," *8th European Symposium on Aerothermodynamics for Space Vehicles*, No. 85751, Lisbon, Portugal, March 2015.

[3] Schrooyen, P., *Numerical simulation of aerothermal flows through ablative thermal protection systems*, Ph.D. thesis, 2015.

[4] Duzel, U. and Martin, A., "Modeling High Velocity Flow Through Porous Media," *AIAA Scitech 2020 Forum*, AIAA Paper 2020-0486, Orlando, Florida, January 2020.

[5] Davuluri, R. S. C., Zhang, H., Tagavi, K. A., and Martin, A., "Effects of spalled particles thermal degradation on a hypersonic flow field environment," *International Journal of Multiphase Flow*, Vol. 159, February 2023, pp. 104287.

[6] Davuluri, R. S. C., Zhang, H., and Martin, A., "Numerical Study of Spallation Phenomenon in an Arc-Jet Environment," *Journal of Thermophysics and Heat Transfer*, Vol. 30, No. 1, jan 2016, pp. 32–41.

[7] Davuluri, R. S. C., Fu, R., Tagavi, K. A., and Martin, A., "Fully coupled material response and internal radiative heat transfer for three-dimensional heat shield modeling," *Journal of Thermophysics and Heat Transfer*, Vol. 38, No. 1, January 2024.

[8] Baeg, S., Davuluri, R., and Martin, A., "Development of two-temperature model in unified solver," *AIAA Scitech 2024 Forum*, AIAA Paper 2024-0445, Orlando, Florida, January 2024.

[9] Gnoffo, P. A., Gupta, R. N., and Shinn, J. L., "Conservation Equations and Physical Models for Hypersonic Air Flows in Thermal and Chemical Nonequilibrium," Technical Paper NASA-TP-2867, NASA, February 1989.

[10] Zhang, H., *High Temperature Flow Solver for Aerothermodynamics Problems*, Ph.d. dissertation, University of Kentucky, Lexington, Kentucky, August 2015.

[11] Park, C., *Nonequilibrium hypersonic aerothermodynamics*, Wiley, New York, 1990.

[12] Anderson, J. D., *Hypersonic and high temperature gas dynamics*, AIAA, 1989.

[13] Vincenti, W. G. and Kruger, C. H., *Introduction to physical gas dynamics*, Wiley, New York, February 1965.

[14] Boyd, I. D. and Josyula, E., "State resolved vibrational relaxation modeling for strongly nonequilibrium flows," *Physics of Fluids*, Vol. 23, No. 5, 2011.

[15] Schroeder, O., "Verification and Validation Studies for the KATS Aerothermodynamics and Material Response Solver," 2018.

[16] Casseau, V., Palharini, R. C., Scanlon, T. J., and Brown, R. E., "A two-temperature open-source CFD model for hypersonic reacting flows, part one: zero-dimensional analysis," *Aerospace*, Vol. 3, No. 4, 2016, pp. 34.